Table 2. *The* Pd–Se *bonds* (Å) *within* 2·58 Å

Pd_7Se_2			
Pd(1[i])–Se	2·434 (2)	Pd(2[ii])–Se	2·532 (2)
Pd(2[iii])–Se	2·467 (2)	Pd(3)–Se	2·576 (2)
Pd(3[ii])–Se	2·462 (2)	Pd(4)–Se	2·462 (2)
Pd(4[i])–Se	2·482 (2)		

Symmetry operations: (i) $\frac{1}{2}-x, -\frac{1}{2}+y, 1-z$; (ii) $\frac{1}{2}-x, -\frac{1}{2}+y, -z$; (iii) $-\frac{1}{2}+x, \frac{3}{2}-y, z$.

$Pd_{34}Se_{11}$			
Pd(1)–Se(1)	2·408 (2)	Pd(2)–Se(1)	2·482 (3)
Pd(3)–Se(1)	2·447 (2)	Pd(1[i])–Se(2)	2·463 (4)
Pd(2)–Se(2)	2·505 (3)	Pd(4[i])–Se(2)	2·407 (3)
Pd(5)–Se(2)	2·404 (4)	Pd(6[i])–Se(2)	2·457 (3)
Pd(13[ii])–Se(2)	2·485 (5)	Pd(16[ii])–Se(2)	2·498 (4)
Pd(4)–Se(3)	2·455 (3)	Pd(7)–Se(3)	2·411 (4)
Pd(8)–Se(3)	2·443 (3)	Pd(9)–Se(3)	2·424 (4)
Pd(9[iii])–Se(3)	2·532 (5)	Pd(6[iv])–Se(4)	2·456 (3)
Pd(7[i])–Se(4)	2·430 (4)	Pd(10[i])–Se(4)	2·406 (3)
Pd(11)–Se(4)	2·428 (4)	Pd(14[i])–Se(4)	2·572 (5)
Pd(3[v])–Se(5)	2·462 (3)	Pd(10[vi])–Se(5)	2·401 (3)
Pd(11)–Se(5)	2·473 (4)	Pd(12)–Se(5)	2·430 (4)
Pd(13)–Se(5)	2·557 (6)	Pd(14)–Se(5)	2·417 (4)
Pd(8[vii])–Se(6)	2·445 (3)	Pd(12[vii])–Se(6)	2·406 (3)
Pd(15)–Se(6)	2·453 (3)	Pd(15[viii])–Se(6)	2·515 (4)
Pd(16)–Se(6)	2·447 (5)	Pd(17)–Se(6)	2·431 (4)

Symmetry operations: (i) $x, -1+y, z$; (ii) $\frac{1}{2}-x, -\frac{1}{2}+y, \frac{1}{2}-z$; (iii) $\frac{1}{2}-x, \frac{1}{2}+y, \frac{3}{2}-z$; (iv) $\frac{1}{2}-x, -\frac{1}{2}+y, \frac{3}{2}-z$; (v) $-\frac{1}{2}+x, \frac{3}{2}-y, -\frac{1}{2}+z$; (vi) $-x, 1-y, 1-z$; (vii) $x, 1+y, z$; (viii) $\frac{1}{2}-x, \frac{1}{2}+y, \frac{1}{2}-z$.

angles of non-linear bonds are between 110·12 (4) and 137·02 (4)°. The numbers of neighboring Pd atoms within 3·2 Å around the individual Pd atoms are: Pd(1) 8, Pd(2) 9, Pd(3) 8 and Pd(4) 9. The Pd–Pd distances range from 2·743 (2) to 3·069 (2) Å.

(II) $Pd_{34}Se_{11}$. We found that the compound formerly characterized as Pd_3Se by Olsen *et al.* (1979) has a composition slightly shifted towards the palladium-rich region as $Pd_{34}Se_{11}$: the powder pattern listed in their report can be interpreted well by our structural data for $Pd_{34}Se_{11}$. The Pd(5) and Pd(17) atoms are bonded to a single Se atom; the rest of the Pd atoms are coordinated by two Se atoms as mentioned above. The number of Pd neighbors is five to seven around the Se atom, and between five and ten within 3·2 Å around Pd. The values of Pd–Se and Pd–Pd bonds are widely distributed in contrast to those of Pd_7Se_2. The average Pd–Se bond length is 2·455 (4) Å. The Pd–Pd distances range between 2·778 (4) and 3·191 (3) Å.

References

COPPENS, P., GURU ROW, T. N., LEUNG, P., STEVENS, E. D., BECKER, P. J. & YANG, Y. W. (1979). *Acta Cryst.* A**35**, 63–72.

GRØNVOLD, F. & RØST, E. (1962). *Acta Cryst.* **15**, 11–13.

International Tables for X-ray Crystallography (1974). Vol. IV. Birmingham: Kynoch Press. (Present distributor Kluwer Academic Publishers, Dordrecht.)

MAIN, P., FISKE, S. J., HULL, S. E., LESSINGER, L., GERMAIN, G., DECLERCQ, J.-P. & WOOLFSON, M. M. (1978). *MULTAN*78. *A System of Computer Programs for the Automatic Solution of Crystal Structures from X-ray Diffraction Data.* Univs. of York, England, and Louvain, Belgium.

MATKOVIĆ, T. & SCHUBERT, K. (1978). *J. Less-Common Met.* **59**, 57–63.

OLSEN, T., RØST, E. & GRØNVOLD, F. (1979). *Acta Chem. Scand. Ser. A*, **33**, 251–256.

SAKURAI, T. (1967). Editor. *UNICS*II. *Universal Crystallographic Computation Program System.* The Crystallographic Society of Japan, Tokyo, Japan.

TAKABATAKE, T., ISHIKAWA, M. & JORDA, J. L. (1987). *J. Less-Common Met.* **134**, 79–89.

TAKABATAKE, T., ISHIKAWA, M. & JUNOD, A. (1988). *J. Phys. Soc. Jpn*, **57**, 2763–2767.

Acta Cryst. (1989). C**45**, 3–7

Oxygen Vacancy Ordering in the Defect Pyrochlore $Pb_2[TiSb]O_{6.5}$: A Rietveld Refinement of Neutron Powder Diffraction Data

BY J. A. ALONSO,* C. CASCALES AND I. RASINES†

Instituto de Ciencia de Materiales, CSIC, Serrano 113, 28006 *Madrid, Spain*

AND J. PANNETIER

Institut Laue Langevin, Avenue des Martyrs, 156 *X,* 38042 *Grenoble CEDEX, France*

(*Received* 5 *May* 1988; *accepted* 9 *August* 1988)

Abstract. $M_r = 688·13$, cubic, $F\bar{4}3m$, $a = 10·4109$ (2) Å, $V = 1128·40$ (6) Å^3, $Z = 8$, $D_x = 8·10$ Mg m^{-3}, neutron powder diffraction (Rietveld method), $\lambda = 1·9109$ Å, $T = 295$ K, $R_p = 5·40$, $R_{wp} = 7·14$, $R_e = 5·48$, $R_I = 1·69\%$ for 52 integrated Bragg intensities, goodness of fit $R_g = 1·70$. Oxygen coordination polyhedra for Ti,Sb are nearly regular octahedra, whereas that for Pb is a scalenohedron with the

* Present address: Centre d'Etudes Nucleaires, DRF/SPhMDN, 85 X, 38041 Grenoble CEDEX, France.

† Author to whom correspondence should be addressed.

0108-2701/89/010003-05$03.00

eighth vertex unoccupied. The Pb atoms are displaced by 0·040 (4) Å along the [111] direction from the ideal $Fd\bar{3}m$ pyrochlore structure, producing small tetrahedral cages [Pb–Pb distances 3·617 (3) Å] inside which the oxygen vacancies show an ordered arrangement.

Introduction. Complex oxides adopting the pyrochlore structure, of general formula $A_2B_2O_6O'$, frequently exhibit partial or total deficiency of the special O′ oxygens. This behaviour can be explained if the structure is viewed as formed of two interpenetrating networks, B_2O_6 and A_2O' (Sleight, 1968), made up of corner-shaped units of BO_6 octahedra, more or less distorted, and A_4O' tetrahedra, respectively. The B_2O_6 network is always more stable than the A_2O' and both do not interact strongly; hence A and O' ions are not essential for the stabilization of the basic structure, and both cationic and anionic vacancies can exist.

A family of defect cubic pyrochlores of stoichiometry $Pb_2(M_pSb_{2-p})O_{6.5}$, where M represents a di-, tri- or tetravalent transition metal, with $p = \frac{1}{3}$, $\frac{1}{2}$ or 1, respectively, has recently been described (Cascales & Rasines, 1986; Cascales, Rasines, García-Casado & Vega, 1985; Cascales, Alonso & Rasines, 1986). In a preliminary X-ray powder diffraction (XRPD) study at room temperature these compounds were described in space group $Fd\bar{3}m$ (No. 227), $Z = 8$ with the origin at $\bar{3}m$, Pb atoms located at 16(c) (0,0,0) positions, M and Sb randomly distributed at 16(d) ($\frac{1}{2}$, $\frac{1}{2}$, $\frac{1}{2}$), the O oxygens at 48(f) (x, $\frac{1}{8}$, $\frac{1}{8}$), and the special O′ oxygens (0·5 per formula) statistically distributed at half the 8(a) positions.

A neutron powder diffraction (NPD) study of the cubic pyrochlore $Pb_2Ru_2O_{6.5}$ (Beyerlein, Horowitz, Longo, Leonowicz, Jorgensen & Rotella, 1984) showed evidence for oxygen vacancy ordering accompanied by A-site displacement. The diffraction data for that compound were successfully fitted in the cubic space group $F\bar{4}3m$.

In order to investigate the vacancy ordering of the above-mentioned Sb-containing pyrochlores, an NPD study of the representative compound $Pb_2[TiSb]O_{6.5}$ has been performed. This paper reports the results of that study.

Experimental. $Pb_2[TiSb]O_{6.5}$ was prepared as a yellow polycrystalline powder from stoichiometric mixtures of analytical grade PbO, TiO_2 and Sb_2O_3, which were heated in air to a final temperature of 1273 K. Details of the synthesis and chemical characterization are given elsewhere (Cascales, Alonso & Rasines, 1986).

The XRPD pattern was collected using a Siemens Kristalloflex 810 generator, Cu $K\alpha$ radiation (λ = 1·540598 Å) and a D 500 goniometer provided with a graphite monochromator, at a scanning rate of 0·1°(2θ) min^{-1}, with tungsten, a = 3·16524 (4) Å, as an internal standard. The a unit-cell parameter was determined from the 2θ values of the last seven reflections of the XRPD diagram. [JCPDS No. 39-1423.]

The NPD pattern was collected at room temperature in the high-resolution diffractometer D1A at the H22 thermal neutron guide of the high-flux reactor of the Institut Laue–Langevin, Grenoble. A neutron wavelength of 1·9109 Å was selected from the (511) planes of a germanium monochromator. D1A is provided with a bank of ten ^{3}He high-pressure counters with a 6° angular separation; the resultant intensity profile is obtained by properly combining the intensities of the counters. The angular range covered was $6° \le 2\theta \le 150°$, scanning in steps of 0·05° (2θ).

The data collection required 16 h. The powdered sample was contained in a cylindrical vanadium can (diameter 15 mm). No precautions to avoid preferred orientation were taken.

The neutron diffraction pattern was analysed by the Rietveld (1969) method, using the Wiles & Young (1982) profile refinement program, which employs a Newton–Raphson algorithm to minimize the function $x = \sum_i w_i[y_i - (1/c)y_{ci}]^2$, where y_i and y_{ci} are the observed and calculated data points, w_i is the statistical weight ($w_i = 1/\sigma_i$) and c is the scale factor.

A Pearson VII function was chosen to generate the line shape of the diffraction peaks. The background was estimated by linear interpolation between points corresponding to regions devoid of reflections. The coherent scattering lengths for Pb, Ti, Sb and O were 9·400, −3·300, 5·641 and 5·805 fm respectively (Koester, Rauch, Herkens & Schröder, 1981).

The following R factors were calculated: the profile $R_p = 100\sum_i |y_i - (1/c)y_{ci}| / \sum_i |y_i|$; the weighted profile $R_{wp} = 100[\sum_i w_i |y_i - (1/c)y_{ci}|^2 / \sum_i w_i |y_i|^2]^{1/2}$; the Bragg $R_I = 100\sum_i |I_i - I_{ic}| / |I_i|$, where I_i, I_{ci} are the observed and calculated integrated intensities; the expected $R_e = 100[(N-P+C)/\sum_i w_i y_i^2]^{1/2}$, where $N-P+C$ is the number of degrees of freedom (N is the number of points in the pattern, P the number of refined parameters and C the number of constraint functions); the goodness of fit $R_g = (R_{wp}/R_e)^2$.

The NPD diagram corresponds to a cubic compound, and shows several weak $hk0$ lines, with $h+k \neq 4n$ (420, 860) and $h00$, with $h \neq 4n$ (200) that could not be detected by XRPD. These lines are forbidden in $Fd\bar{3}m$, and are consistent with the loss of inversion symmetry at the cation sites, a result that would occur if the oxygen vacancies (4 per unit cell) were ordered (Beyerlein, Horowitz, Longo, Leonowicz, Jorgensen & Rotella, 1984). The profile refinement was performed in the noncentrosymmetric space group $F\bar{4}3m$ (No. 216), that allows us to set up a model which accounts for this ordering. In this space group cation displacement along [111] is also allowed. All the cations were placed at 16(e) (x, x, x) sites, O1 at 24(f)

Table 1. *Atomic positions, occupancy factors, equivalent isotropic and anisotropic thermal parameters* (Å^2) *with e.s.d.'s in parentheses for* $Pb_2[TiSb]O_{6.5}$ *at* 295 K

$B_{eq} = 4a^2\beta_{11}$ (B_{iso} for [Ti,Sb]).

	Site	x	y	z	Occupancy	B_{eq}	β_{11}	β_{22}	β_{33}	β_{12}	β_{13}	β_{23}
Pb	16 (*e*)	0·8728 (3)	x	x	0·983 (5)	1·20 (3)	0·00277 (7)		β_{11}	−0·00055 (8)	β_{12}	β_{12}
Ti/Sb	16 (*e*)	0·3747 (19)	x	x	0·5	0·10 (13)						
O1	24 (*f*)	0·3051 (3)	0	0	1	0·81 (4)	0·00187 (10)	0·00153 (7)	β_{22}	0	0	−0·00016 (38)
O2	24 (*g*)	0·0565 (3)	¼	¼	1	0·81 (4)	0·00187 (10)	0·00153 (7)	β_{22}	0	0	−0·00016 (38)
O3	4 (*a*)	0	0	0	0·997 (14)	1·41 (16)	0·00325 (38)	β_{11}	β_{11}	0	0	0

(x, 0, 0), O2 at 24(g) (x, ¼, ¼), and O3 (O′ in $A_2B_2O_6O'_{0.5}$) at 4(a) (0, 0, 0). Sb and Ti atoms were considered to be statistically distributed [1:1] over the same crystallographic positions. The atomic positional parameters taken in the starting model in $F\bar{4}3m$ were those determined by XRPD in $Fd\bar{3}m$ (Cascales, Alonso & Rasines, 1986) transformed by means of the relationship

$$\begin{pmatrix} x \\ y \\ z \end{pmatrix}_{F\bar{4}3m} = \begin{pmatrix} x \\ y \\ z \end{pmatrix}_{Fd\bar{3}m} - \begin{pmatrix} \frac{1}{8} \\ \frac{1}{8} \\ \frac{1}{8} \end{pmatrix}.$$

The thermal factors for O1 and O2 were constrained; otherwise, the refinement led to negative thermal factors for [Ti,Sb].

No regions were excluded in the refinement. Since the presence of small amounts of TiO_2 (rutile) was detected in the pattern, the profile refinement of the mixture was performed. Structural parameters for TiO_2, taken from Cronschorek (1982), were not refined. 28 parameters were refined, including background coefficients; zero-point; half-width, Pearson and asymmetry parameters for the peak shape; independent scale factors for TiO_2 and $Pb_2[TiSb]O_{6.5}$; positional, thermal, unit-cell parameters and Pb and O′ occupancy factors for the pyrochlore phase. Owing to the small contribution of Ti/Sb atoms on site 16(e) to the diffracted intensities $\langle b \rangle = \frac{1}{2}[b(\mathrm{Ti}) + b(\mathrm{Sb})] = 1{\cdot}171$ fm, anisotropic thermal factors for this site were not refined. The maximum value for Δ/σ in the final refinement cycle was 0·11.

From the refined scale factors of the rutile and pyrochlore phases, a molar ratio of TiO_2:$Pb_2[TiSb]O_{6.5}$ = 0·016:1 was calculated for the mixture.

Discussion. Final positional and anisotropic thermal parameters are given in Table 1, and selected internuclear distances are listed in Table 2. The agreement between the observed and calculated profile is shown in Fig. 1.* The structure is basically the same as that found by XRPD (Cascales, Alonso & Rasines, 1986). The refined position parameters for the O1 and O2 atoms [average $Fd\bar{3}m$ equivalent value x(O) = 0·4315 (3)] agree with the reported XRPD value, x(O) = 0·433. For such an oxygen parameter, close to 0·4375, the oxygen polyhedra around Ti,Sb atoms are slightly distorted octahedra (Subramanian, Aravamudan & Subba Rao, 1983). The refined occupancy factor for the oxygen at 4(a), 0·997 (14), yielding a stoichiometry of 0·499 (7), confirms the half deficiency of the O′ atom in this pyrochlore-type compound.

The refined positional parameter for the [Ti,Sb] atoms, 0·3747 (17), is within 1 standard deviation of

Table 2. *Selected interatomic distances* (Å) *with e.s.d.'s in parentheses at* 295 K

$[Ti,Sb]O_6$ octahedra		□Pb_4 tetrahedra	
[Ti,Sb]–O1	1·982 (20) × 3	□–Pb	2·215 (3) × 4
[Ti,Sb]–O2	1·966 (20) × 3	Pb–Pb	3·617 (3) × 3
PbO_7 scalenohedra		O′Pb_4 tetrahedra	
Pb–O1	2·634 (4) × 3	O3–Pb	2·294 (3) × 4
Pb–O2	2·643 (4) × 3	Pb–Pb	2·746 (3) × 3
Pb–O3	2·294 (3) × 1		

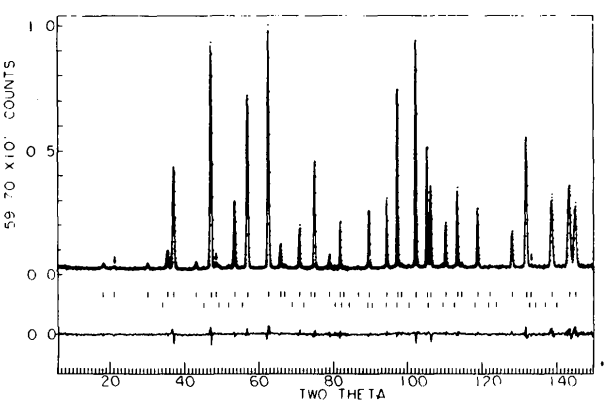

Fig. 1. Neutron diffraction profile at 295 K. Crosses are the raw data points, the solid line is the best fit profile. The difference plot (observed–calculated) appears at the bottom. The two series of thick marks below the profile indicate the positions of all the allowed reflections included in the calculation, for the phases $Pb_2[TiSb]O_{6.5}$ (upper series) and TiO_2, rutile (lower series). Small arrows indicate the reflections forbidden in $Fd\bar{3}m$.

* The measured intensity as a function of the scattering angle and a list of integrated intensities for both $Pb_2[TiSb]O_{6.5}$ and TiO_2 phases have been deposited with the British Library Document Supply Centre as Supplementary Publication No. SUP 51320 (11 pp.). Copies may be obtained through The Executive Secretary, International Union of Crystallography, 5 Abbey Square, Chester CH1 2HU, England.

the value corresponding to the $Fd\bar{3}m$ inversion position, $x = 0{\cdot}375$; hence this displacement should not be considered as significant. The high values of the e.s.d.'s obtained for [Ti,Sb] in both positional and thermal isotropic parameters could be attributed to the small scattering length resulting from the random distribution of Ti and Sb, which have individual lengths of opposite sign. These high values could also represent slightly different sites for Ti and for Sb in their disordered distribution.

The Pb atoms are coordinated to seven oxygens, 3 O1, 3 O2 and 1 O3, placed at the vertices of a scalenohedron, whose eighth vertex remains unoccupied (Fig. 2). The refined positional parameter for Pb, $x(Pb) = 0{\cdot}8728$ (3), shows that this atom is significantly shifted from the $Fd\bar{3}m$ inversion position ($x = 0{\cdot}875$). The Pb atoms are displaced along the [111] direction towards the closest oxygen vacancy, in such a way that each vacancy is inside a tetrahedral cage constituted by four lead atoms, the Pb—O vacancy distances being 2·215 (3) Å, whereas Pb—O′ distances in $O'Pb_4$ tetrahedra are 2·294 (3) Å. Fig. 3 shows a polyhedral projection of the structure, in which the $A_2O'_{0.5}$ sublattice has been emphasized. It shows the ordered alternation of two different-sized perfect tetrahedra, $\square Pb_4$ and $O'Pb_4$, the former of smaller size. The refined occupancy factor of Pb, yielding a stoichiometry of 1·966 (10), shows a slight deficiency of this element, probably due to volatilization during synthesis.

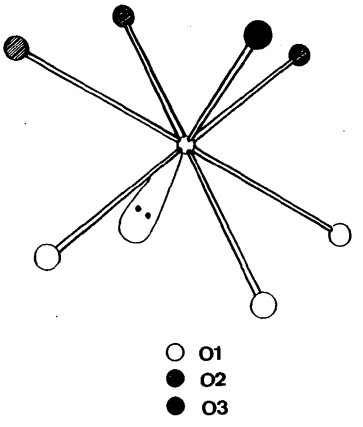

Fig. 2. Oxygen coordination polyhedron for Pb atoms.

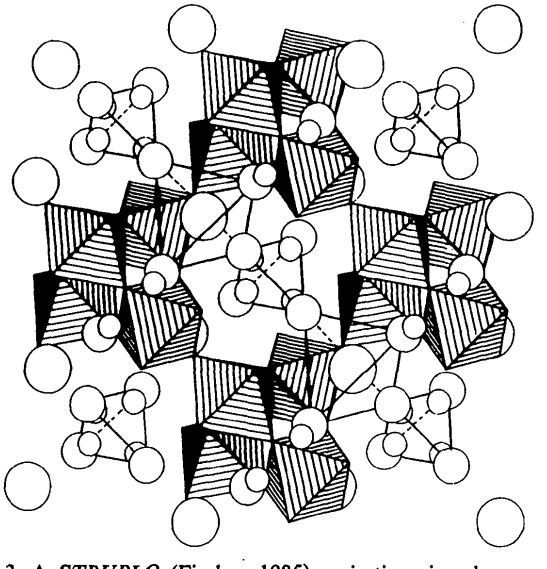

Fig. 3. A *STRUPLO* (Fischer, 1985) projection viewed approximately along the [001] direction. Large circles represent O′ oxygens, medium and small circles represent Pb atoms and their associated electron pairs, respectively. The small $\square Pb_4$ tetrahedra are suggested to lodge the four electron pairs of the Pb^{II} cations comprising them. For the sake of clarity, the atomic displacement of Pb has been enhanced.

The displacement of Pb can be explained as a consequence of the electrostatic repulsion between the nonbonded Pb^{II} lone pair and the Pb—O bonds of its own coordination polyhedron, implying that the lone pair is directed towards the oxygen vacancy (Fig. 2). It can be suggested that the vacancy sites, special positions 4(*c*) ($\frac{3}{4}$, $\frac{3}{4}$, $\frac{3}{4}$), are actually, occupied by the electron pairs of the four Pb atoms associated with each one. Therefore, the stereochemical influence of the Pb^{II} inert pair would determine the oxygen deficiency of this compound and probably that of all the family of Pb/Sb pyrochlores.

The successful fit of the neutron diffraction data of $Pb_2[TiSb]O_{6.5}$ in the space group $F\bar{4}3m$ demonstrates oxygen vacancy ordering for this compound, and supports the suggestion of Beyerlein, Horowitz, Leonowicz, Jorgensen & Rotella (1984) that this kind of ordering may be a frequently encountered phenomenon for oxygen defect pyrochlores with post-transition-metal cations such as Tl^+, Pb^{2+} or Bi^{3+} on the *A* site.

The authors acknowledge the receipt of two postdoctoral fellowships (JAA and CC) and the financial aid of the Consejo Superior de Investigaciones Cientificas. They thank the ILL for making all facilities available.

References

BEYERLEIN, R. A., HOROWITZ, H. S., LONGO, J. M., LEONOWICZ, M. E., JORGENSEN, J. A. & ROTELLA, F. J. (1984). *J. Solid State Chem.* **51**, 253–265.

CASCALES, C., ALONSO, J. A. & RASINES, I. (1986). *J. Mater. Sci. Lett.* **5**, 675–677.

CASCALES, C. & RASINES, I. (1986). *J. Chem. Soc. Dalton Trans.* pp. 1247–1249.

CASCALES, C., RASINES, I., GARCÍA-CASADO, P. & VEGA, J. (1985). *Mater. Res. Bull.* **20**, 1359–1365.

CRONSCHOREK, W. (1982). *Z. Kristallogr.* **160**, 187–203.

FISCHER, R. X. (1985). *J. Appl. Cryst.* **18**, 258–262.

KOESTER, L., RAUCH, H., HERKENS, M. & SCHRÖDER, K. (1981). Report 1755. Kernforschungsanlage Jülich, Federal Republic of Germany.
RIETVELD, H. H. (1969). *J. Appl. Cryst.* **2**, 65–71.
SLEIGHT, A. W. (1968). *Inorg. Chem.* **7**, 1704.
SUBRAMANIAN, M. A., ARAVAMUDAN, G. & SUBBA RAO, G. V. (1983). *Prog. Solid State Chem.* **15**, 55–143.
WILES, D. B. & YOUNG, R. A. (1982). *J. Appl. Cryst.* **15**, 430–438.

Acta Cryst. (1989). C**45**, 7–11

Structures of Nitrato[*N*-(2-pyridylmethyl)salicylideneaminato-*N*,*O*]copper(II), [Cu(salimp)NO_3], and Dichloro[*N*-(2-pyridylmethyl)salicylamine-*N*,*N'*]copper(II)–Methanol–Water (1/1/1), [Cu(Hsalamp)Cl_2].$CH_3OH.H_2O$

BY JEAN-MARC LATOUR AND SANTOKH SINGH TANDON*

Laboratoires de Chimie, DRF, CENG, 85X, F-38041 Grenoble CEDEX, France

AND DAVID C. POVEY†

Department of Chemistry, University of Surrey, Guildford, Surrey GU2 5XH, England

(*Received* 2 *September* 1987; *accepted* 17 *August* 1988)

Abstract. (I) [Cu($C_{13}H_{11}N_2O$)NO_3], $M_r = 336{\cdot}80$, monoclinic, Pn, $a = 7{\cdot}770$ (1), $b = 5{\cdot}958$ (1), $c = 14{\cdot}403$ (2) Å, $\beta = 101{\cdot}99$ (1)°, $V = 652{\cdot}2$ (3) Å^3, $Z = 2$, $D_x = 1{\cdot}716$ Mg m^{-3}, Mo $K\alpha$, $\lambda = 0{\cdot}71069$ Å, $\mu = 1{\cdot}70$ mm^{-1}, $F(000) = 342$, $T = 292$ K, $R = 0{\cdot}023$ for 1099 observed data with $I \geq 2{\cdot}5\sigma(I)$. (II) [Cu($C_{13}H_{14}N_2O$)$Cl_2$].$CH_4O.H_2O$, $M_r = 398{\cdot}77$, monoclinic, $P2_1/c$, $a = 9{\cdot}959$ (1), $b = 9{\cdot}924$ (1), $c = 18{\cdot}197$ (2) Å, $\beta = 103{\cdot}20$ (2)°, $V = 1751{\cdot}1$ (6) Å^3, $Z = 4$, $D_x = 1{\cdot}51$ Mg m^{-3}, Mo $K\alpha$, $\lambda = 0{\cdot}71069$ Å, $\mu = 1{\cdot}56$ mm^{-1}, $F(000) = 820$, $T = 292$ K, $R = 0{\cdot}037$ for 2377 observed data with $I \geq 3{\cdot}0\sigma(I)$. In (I), the Cu atom is four-coordinate in an essentially square-planar arrangement with the ligand occupying three of the coordination positions. The fourth position is occupied by an O atom of the nitrate group, the plane of which is at an angle of 87·1 (7)° to the best plane through the remainder of the molecule. This allows a second O atom from this group to make a significant contact with the Cu atom thus increasing its coordination number to five in a pseudo-square-pyramidal arrangement. In (II), a similar situation arises with the initial square-planar coordination sphere of two N atoms from the ligand and two Cl atoms being again modified by a further Cl atom, this time from an adjacent molecule.

Introduction. Copper complexes of bi- and tetradentate ligands formed from salicylaldehyde and various mono- or polyamines have been widely studied over the past three decades (Holm, Everett & Chakravorty, 1966; Sinn & Harris, 1969). Considerably less attention has been devoted, however, to copper complexes of tridentate Schiff bases, especially those involving a diamine in addition to the salicyl moiety. This is rather surprising since copper complexes of such ligands can be envisaged as valuable models for the so-called type II copper found in galactose oxidase (Ettinger & Kosman, 1981) or dopamine hydroxylase (Villafranca, 1981) and the mononuclear copper site of metapohaemocyanin (Himmelwright, Eickman & Solomon, 1979).

Copper complexes of ligands formed from salicylaldehyde and *N*-substituted ethylenediamines were first reported 20 years ago (Sacconi & Bertini, 1966). A number of authors have extended these studies more recently (Chieh & Palenik, 1972; Muto & Tokii, 1978; Elias, Hims & Paulus, 1982; Mandal & Nag, 1984). On the other hand, ligands involving only imine N atoms to mimic more closely the histidine coordination have been developed only in the past few years (Nakao, Mori, Okuda & Nakahara, 1979; Wagner & Walker, 1983; Taylor & Coleman, 1982).

In order to obtain a deeper insight into the properties of biological monocopper sites, we started a systematic investigation of copper complexes of ligands resulting from the condensation of salicylaldehyde with an aminoalkylpyridine. In this contribution we describe the crystal structures of two such compounds: the copper nitrate derivative of 2-(2-pyridylmethyliminomethyl)-phenol, (I), and the dichlorocopper complex of 2-(2-pyridylmethylaminomethyl)phenol, (II).

* Present address: Department of Chemistry, Guru Nanak Dev University, Amritsar – 143005, India.
† To whom all correspondence should be addressed.

0108-2701/89/010007-05$03.00